Supplementary data for

Roles of Serum Amyloid A 1 Protein Isoforms in Rheumatoid Arthritis

Elaine Lai-Han Leung [a,#], Huan-Ling Lai [a,#], Run-Ze Li [a], Hu-Dan Pan [a], Ze-Bo Jiang [a], Ying Li [b], Fu-Gang Duan [a], Jia-Hui Xu [a], Yi-Zhong Zhang [a], A-Xi Shi [a], Chun-Li Wei [a], Fang-Yuan Zhang [a], Xiao-Jun Yao [a], Liang Liu [a,*]

[a] *State Key Laboratory of Quality Research in Chinese Medicine & Macau Institute for Applied Research in Medicine and Health & Faculty of Chinese Medicine, Macau University of Science and Technology, Macao 999078, China*

[b] *Department of Pediatrics, Pennsylvania State University College of Medicine, Hershey, PA 17033, USA*

Table S1

Primer design for RT-PCR studies.

Primer	Sequence (5' to 3')
H-SAA-1 F	TTTCTGCTCCTTGGTCCT
H-SAA-1 R	CAGGTCGGAAGTGATTGG
M-TNF-α F	AGCGAGGACAGCAAGGGA
M-TNF-α R	TCTTTTCTGGAGGGAGTGTGG
M-IL-1β F	TTGACGGACCCCAAAAGATG
M-IL-1β R	AGAAGGTGCTCATGTCCTCA
M-IL-6 F	GGTGACAACCACGGCCTTCCC
M-IL-6 R	AAGCCTCCGACTTGTGAAGTGGT
M-IL-22 F	AGCAAATCAGCTCAGCTCCTG
M-IL-22 R	CTTCTTCTCGCTCAGACGCA
M-MMP-3 F	ACATGGAGACTTTGTCCCTTTTG
M-MMP-3 R	TTGGCTGAGTGGTAGAGTCCC
M-MMP-9 F	TGAATCAGCTGGCTTTTGTG
M-MMP-9 R	ACCTTCCAGTAGGGGCAACT
M-G-CSF F	CCCACCTTGGACTTGCTTCAG
M-G-CSF R	AGGTACGAAATGGCCAGGACAC
M-TIMP-1 F	CTTGGTTCCCTGGCGTACTC
M-TIMP-1 R	ACCTGATCCGTCCACAAACAG
M-GAPDH F	TTTGTCGTCCTTGTCAACAGC
M-GAPDH R	CTGGGGAGTTTCAGGTTCCT

TNF: tumor necrosis factor; IL: interleukin; MMP: matrix metalloproteinase; G-CSF: granulocyte-colony stimulating factor; TIMP: tissue inhibitor of metalloproteinases; GADPH: glyceraldehyde-3-phosphate dehydrogenase.

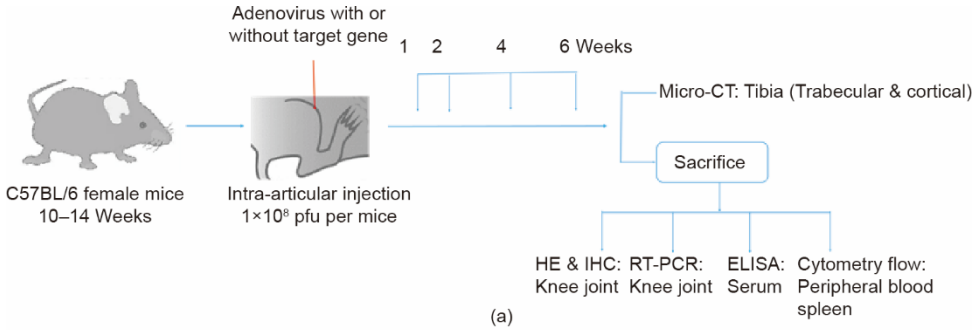

(a)

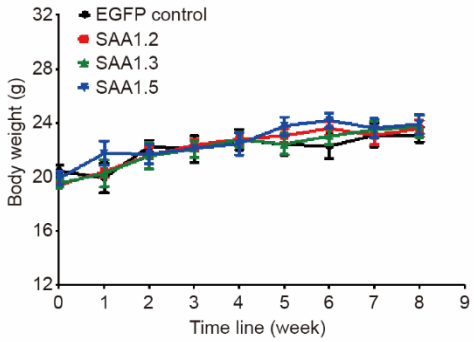

(b)

Fig. S1. (a) Timeline of *in vivo* experiments in this study. (b) Body weight of mice in three SAA 1 groups compared with EGFP control group after modeling adenovirus infection.

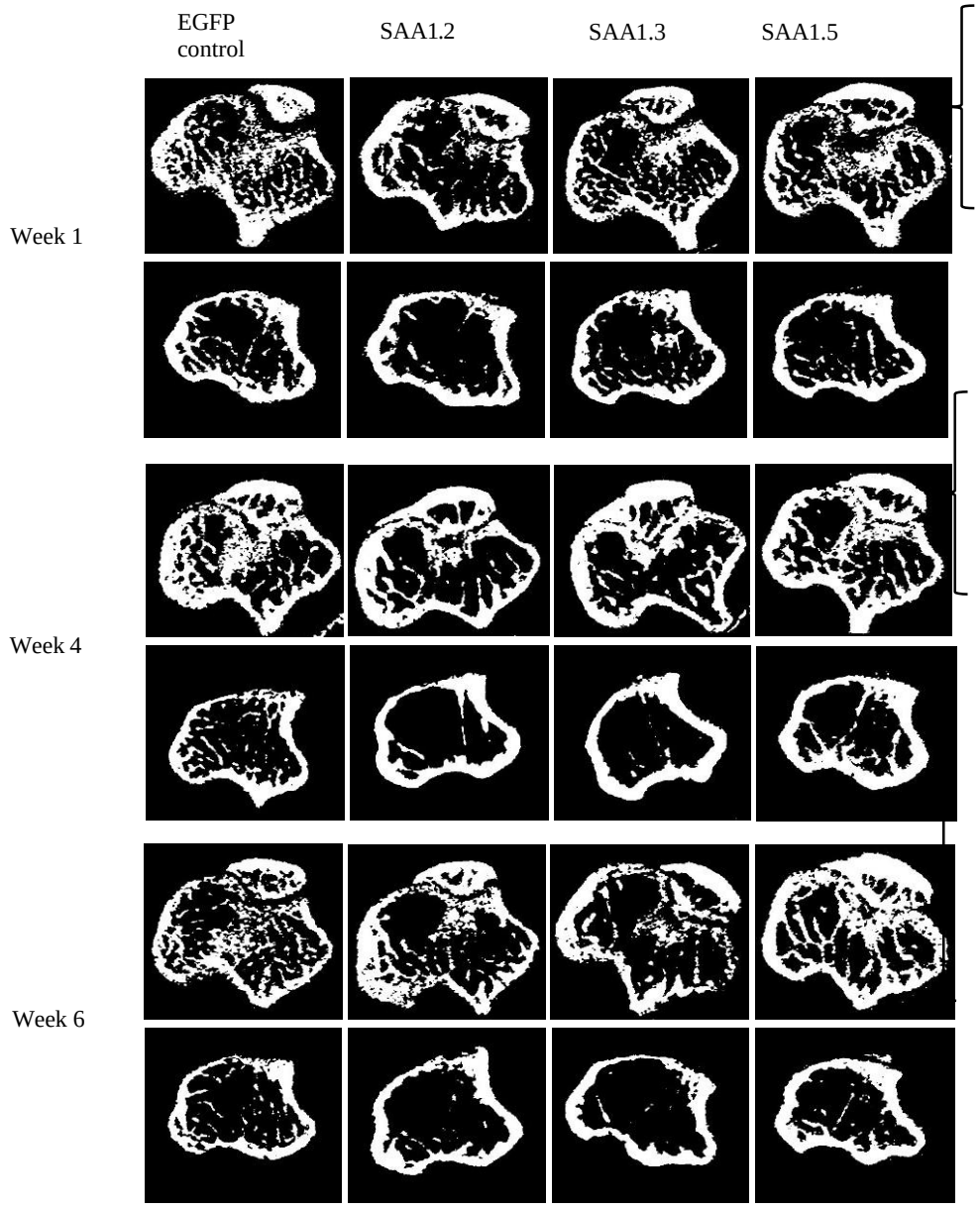

Fig. S2. Micro-CT reconstructed bone images of knee joints for three SAA1 isoforms and the EGFP control group.

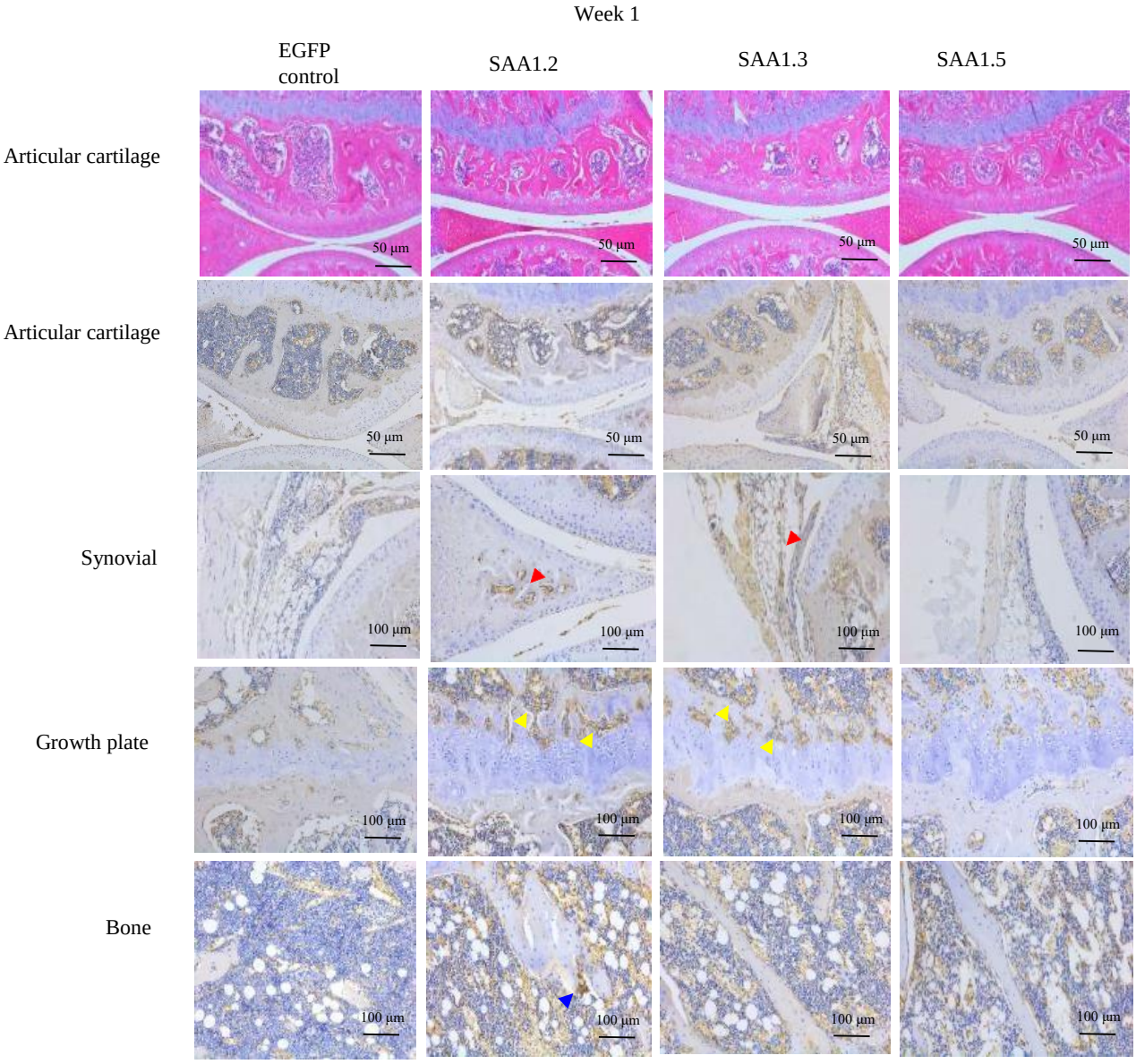

Fig. S3. Overexpression of SAA1 isoforms induces synovial inflammation and adenoviral-SAA1 infects multiple tissues in right knee joints. Tissue harvested at week 1 after modeling infection, hematoxylin and eosin staining of articular cartilage and IHC analysis of localization of SAA1 in different tissues of right knee joints. (The red arrow indicates positive expression of SAA1 in synovial cells, the yellow arrow indicates expression of SAA1 in the growth plate, and the blue arrow represents expression in bone tissue.)

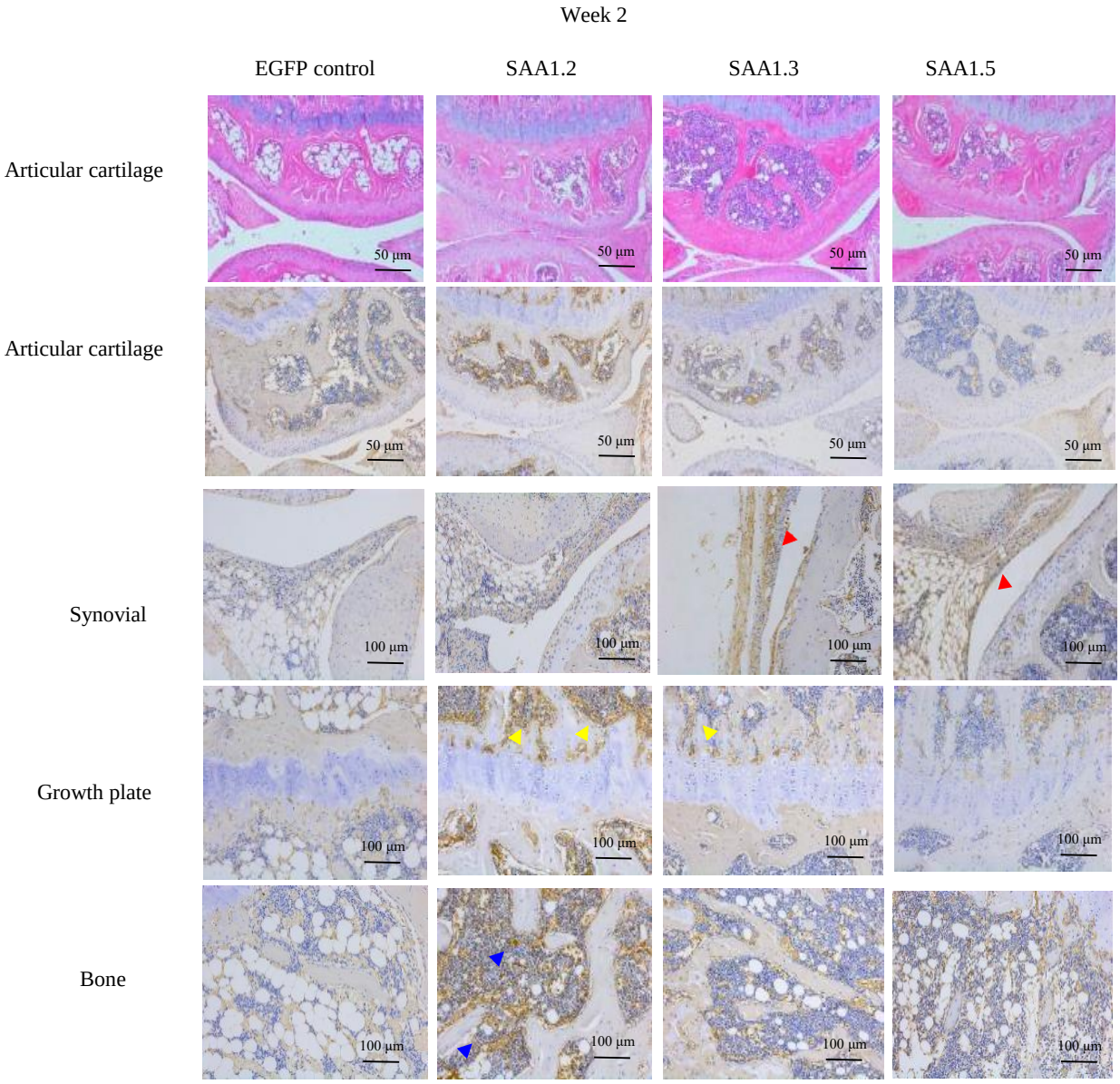

Fig. S4. Overexpression of SAA1 isoforms induces synovial inflammation and adenoviral-SAA1 infects multiple tissues in right knee joints. Tissue harvested at week 2 after modeling infection, hematoxylin and eosin staining of articular cartilage and IHC analysis of localization of SAA1 in different tissues of right knee joints. (The red arrow indicates positive expression of SAA1 in synovial cells, the yellow arrow indicates expression of SAA1 in the growth plate, and the blue arrow represents expression in bone tissue.)

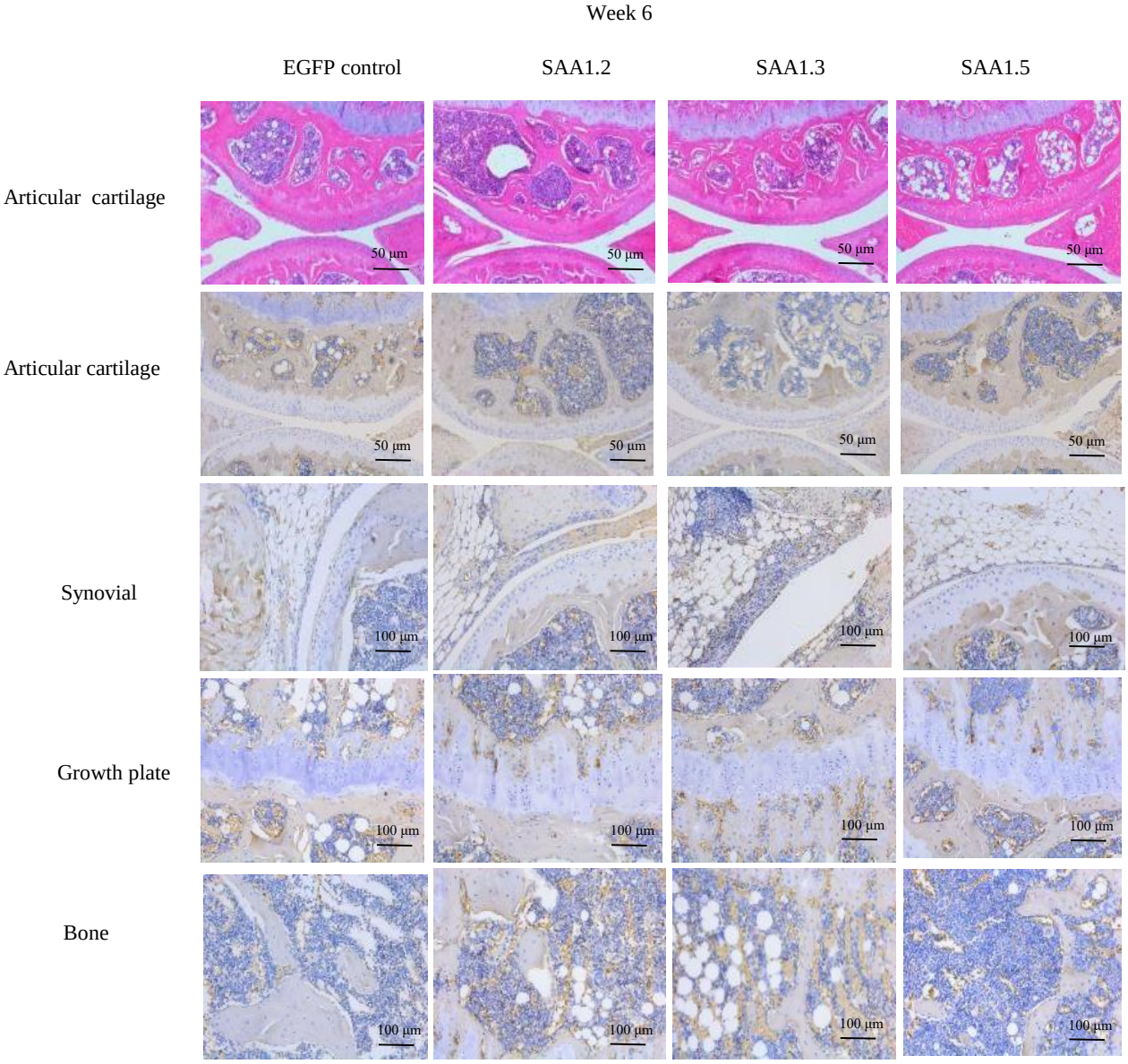

Fig. S5. Overexpression of SAA1 isoforms induces synovial inflammation and adenoviral-SAA1 infects multiple tissues in right knee joints. Tissue harvested at week 6 after modeling infection, hematoxylin and eosin staining of articular cartilage and IHC analysis of localization of SAA1 in different tissues of right knee joints.

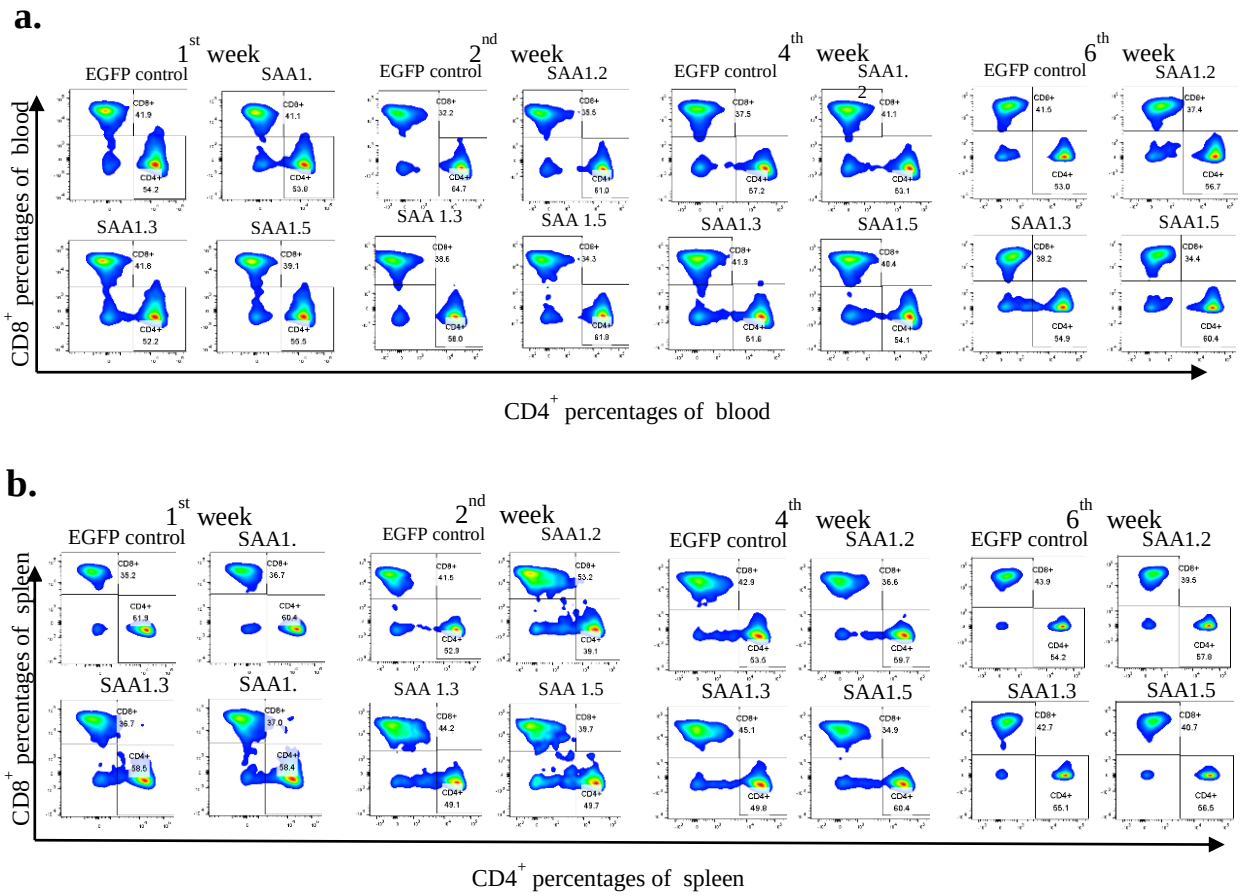

Fig. S6. SAA1 isoforms induced T cell-mediated immune responses. (a) Flow cytometric analysis of the percentages of $CD4^+$ and $CD8^+$ T cells and the fold changes of the $CD8^+/CD4^+$ ratio in the spleen and blood in the SAA1 groups compared with the EGFP group at four different time points. (b) Flow cytometry analysis of the percentage of $CD4^+$ and $CD8^+$ T cells of blood and spleen in three SAA1 groups compared with the EGFP group at four different time points.

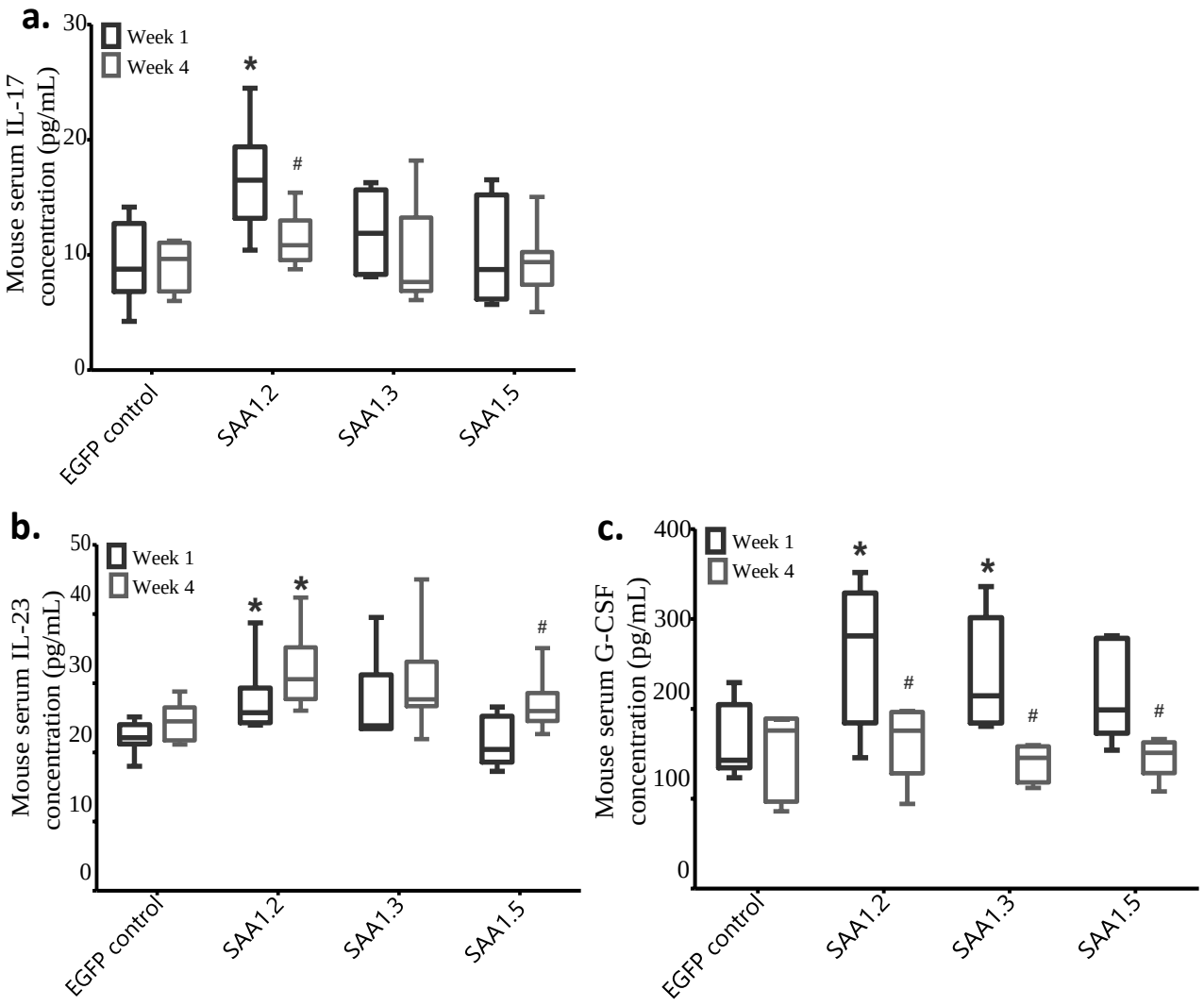

Fig. S7. SAA1 isoforms induced pro-inflammatory cytokines release in blood circulation. ELISA analysis of the secretion of cytokines, IL-17, IL-23, and G-CSF in serum week 1, and week 4 after SAA1 adenoviral infection compared with the EGFP group (n = 6–8 in each group). (a) Mouse serum IL-17 concentration in each group; (b) mouse serum IL-23 concentration in each group; (c) mouse serum G-CSF concentration in each group. *: the p-value for the comparison of value of each *SAA1* allele to the EGFP group; #: the p-value for the value change of each *SAA1* allele over time. *, # $p < 0.05$; **, ## $p < 0.01$; ***, ### $p < 0.001$. Values are presented as the mean ± SEM.

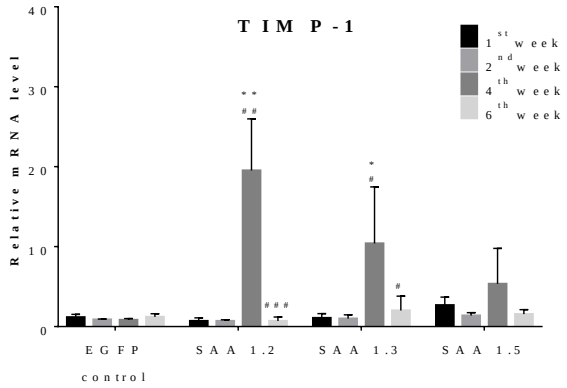

Fig. S8. SAA1 isoforms induced pro-inflammatory cytokines, TIMP-1 related mRNA expression in right articular joints (n = 5–6 in each group). Values are presented as the mean ± SEM.

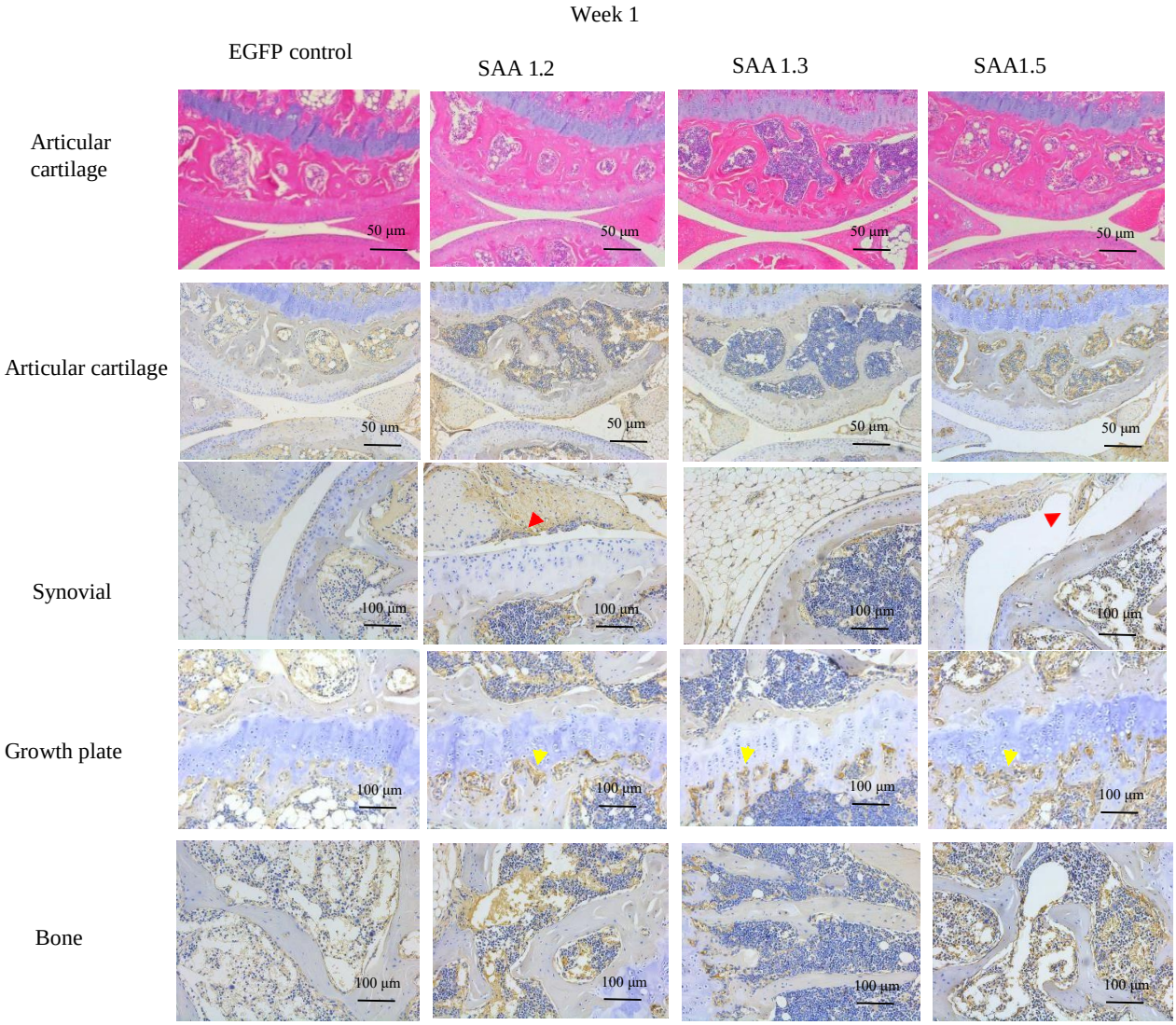

Fig. S9. Overexpression of SAA1 isoforms induces synovial inflammation and adenoviral-SAA1 infects multiple tissues in left knee joints. Tissue harvested at week 1 after modeling infection, hematoxylin and eosin staining of articular cartilage and IHC analysis of localization of SAA1 in different tissues of left knee joints. The red arrow indicates positive expression of SAA1 in synovial cells; the yellow arrow indicates expression of SAA1 in the growth plate.

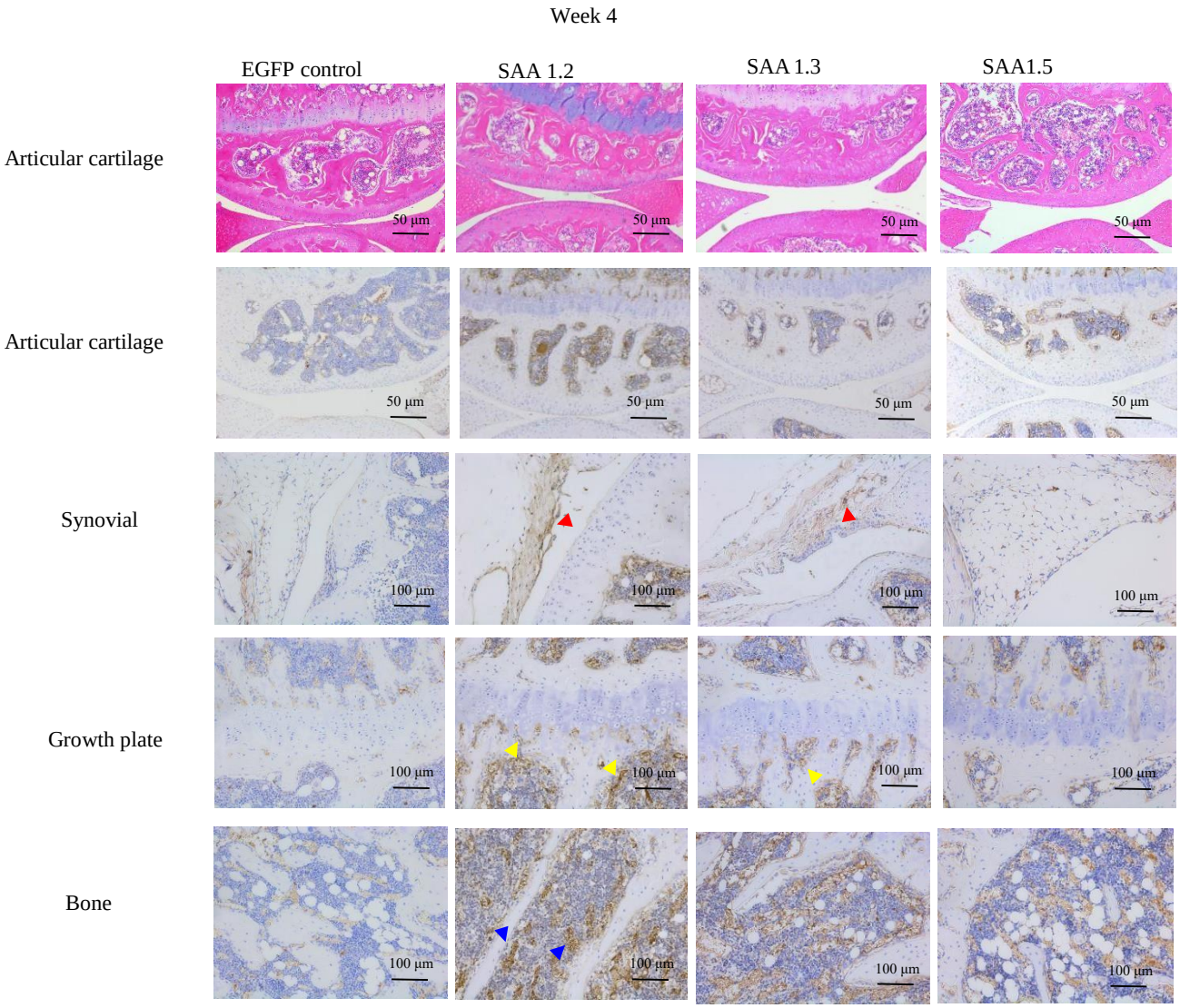

Fig. S10. Overexpression of SAA1 isoforms induces synovial inflammation and adenoviral-SAA1 infects multiple tissues in left knee joints. Tissue harvested at week 4 after modeling infection, hematoxylin and eosin staining of articular cartilage and IHC analysis of localization of SAA1 in different tissues of left knee joints. The red arrow indicates positive expression of SAA1 in synovial cells; the yellow arrow indicates expression of SAA1 in the growth plate; and the blue arrow represents expression in bone tissue.

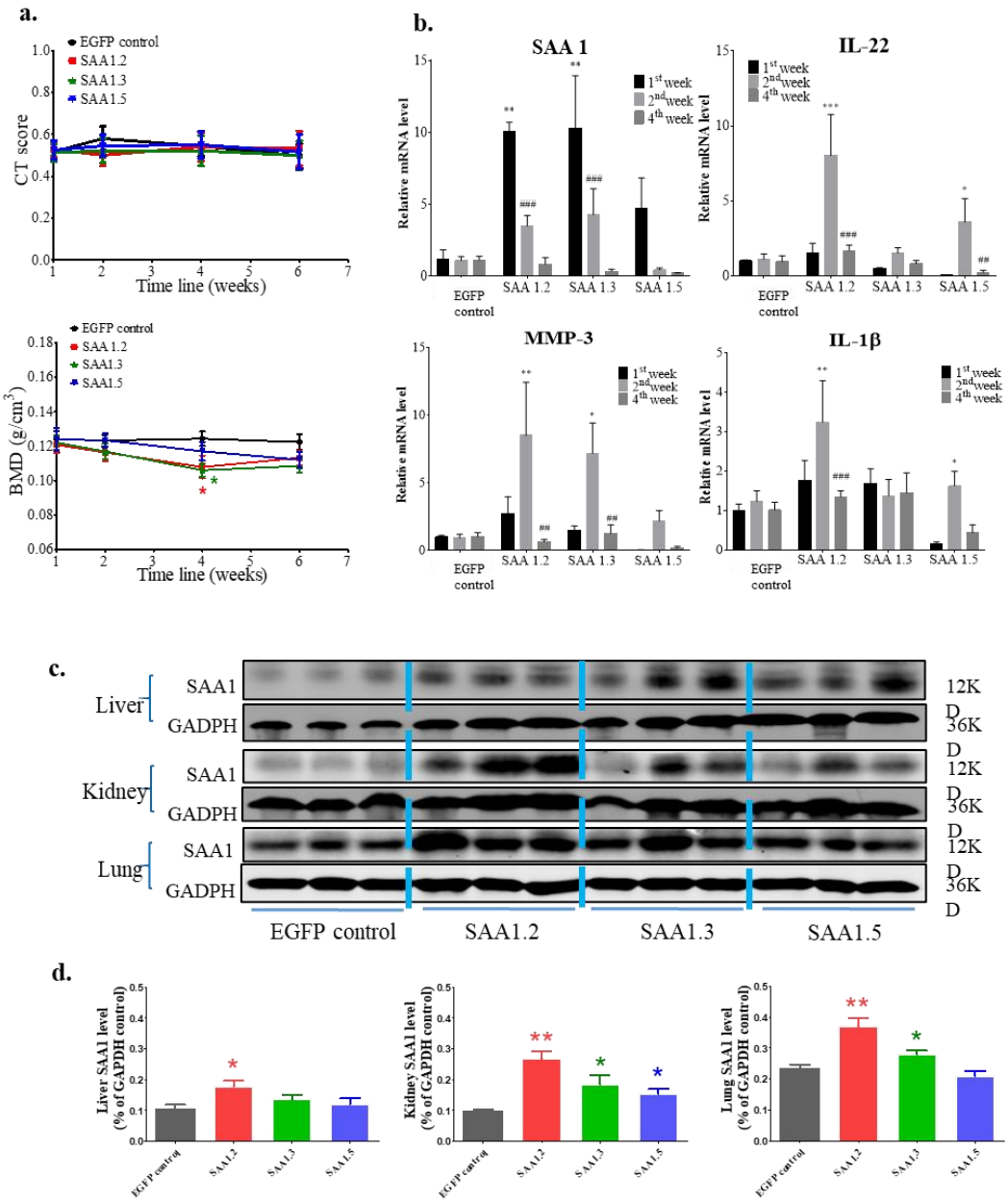

Fig. S11. Systemic effect induced by SAA1 isoforms. (a) Trend changes in CT scores and BMD values of left knee joints over the time course for three SAA1 isoforms compared with the EGFP control group (n = 8 in each group). (b) RT-PCR analysis of the expression of SAA1 and cytokines IL-22, IL-1β, and MMP-3 in left knee joints at week 1, 2, 4, and 6 after SAA1 adenoviral infection compared with the EGFP group (n = 5 in each group). (c) Immunoblots for SAA1 expression in liver, kidney, and lung from mice of EGFP control, SAA1.2, SAA1.3, and SAA1.5 groups. (d) Quantification of the SAA1 level of liver, kidney, and lung determined by western blot analysis (n = 5–6 in each group). Values are presented as the mean ± SEM.

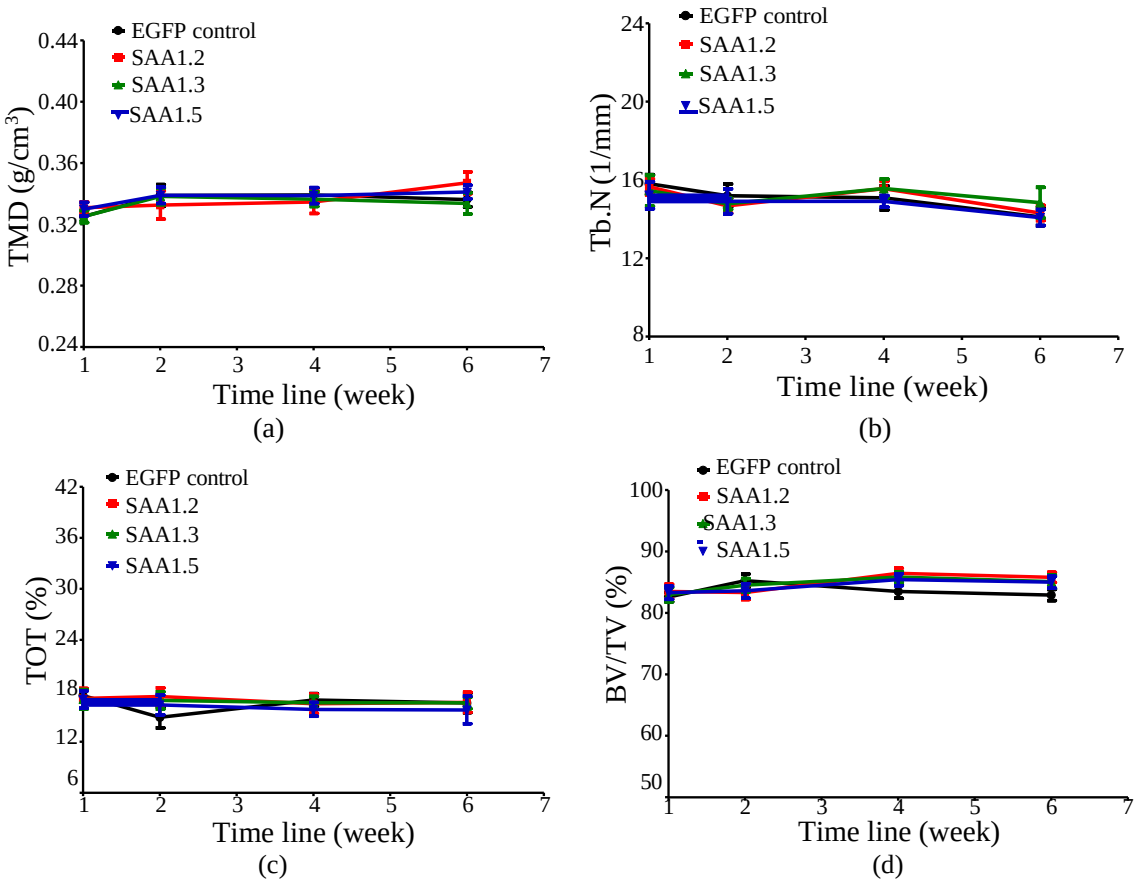

Fig. S12. Qualitative analysis of bone changes of Left side of mice by Micro-CT (n = 8). (a) TMD; (b) trabecular number (Tb.N); (c) total porosity (TOT); and (d) the trabecular volume rate (BV/TV). * $p < 0.05$.

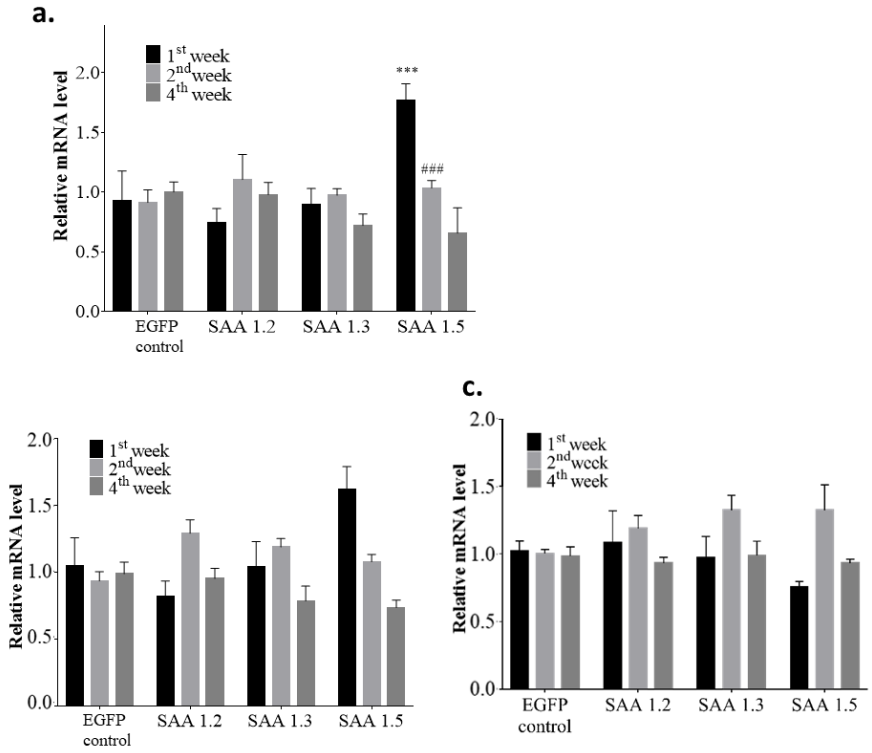

Fig. S13. RT-PCR analysis of the mRNA levels of left knee joints after adenoviral-SAA isoforms transfections (n = 4 in each group). (a) MMP-9; (b) TNF-α; and (c) IL-6. Values are presented as the mean ± SEM.

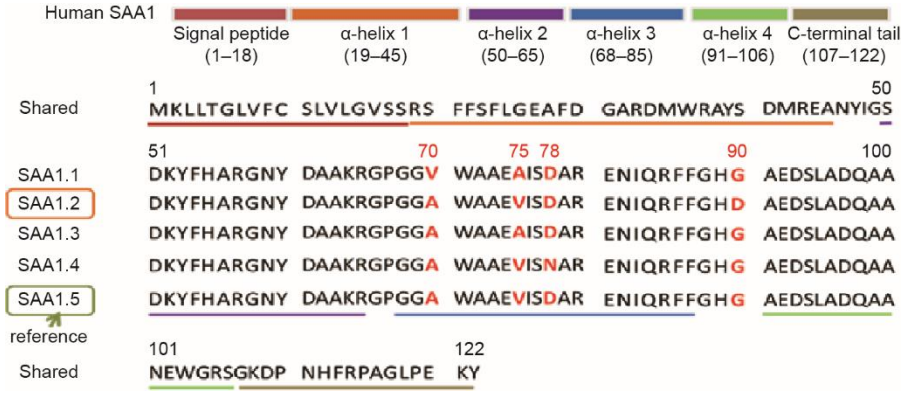

Fig. S14. The protein sequence alignments of SAA1.1, SAA1.2, SAA1.3, SAA1.4, and SAA1.5 encode a few amino acid differences in the protein structure.